Dossier

This paper is a part of the hereunder thematic dossier published in OGST Journal, Vol. 70, No. 1, pp. 3-211 and available online here

Cet article fait partie du dossier thématique ci-dessous publié dans la revue OGST, Vol. 70, n°1, pp. 3-211 et téléchargeable ici

DOSSIER Edited by/Sous la direction de : **B. Leduc et P. Tona**

IFP Energies nouvelles International Conference / Les Rencontres Scientifiques d'IFP Energies nouvelles
E-COSM'12 — IFAC Workshop on Engine and Powertrain Control, Simulation and Modeling
E-COSM'12 — Séminaire de l'IFAC sur le contrôle, la simulation et la modélisation des moteurs et groupes moto-propulseurs

Oil & Gas Science and Technology – Rev. IFP Energies nouvelles, Vol. 70 (2015), No. 1, pp. 3-211

3 > Editorial
B. Leduc and P. Tona

15 > *A Challenging Future for the IC Engine: New Technologies and the Control Role*
Un challenge pour le futur du moteur à combustion interne : nouvelles technologies et rôle du contrôle moteur
F. Payri, J. M. Luján, C. Guardiola and B. Pla

31 > *The Art of Control Engineering: Science Meets Industrial Reality*
L'art du génie automatique : science en rencontre avec la réalité industrielle
U. Christen and R. Busch

41 > *Energy Management of Hybrid Electric Vehicles: 15 Years of Development at the Ohio State University*
Gestion énergétique des véhicules hybrides électriques : 15 ans de développement à l'université d'État de l'Ohio
G. Rizzoni and S. Onori

55 > *Automotive Catalyst State Diagnosis using Microwaves*
Diagnostic de l'état de catalyseurs d'automobiles à l'aide de micro-ondes
R. Moos and G. Fischerauer

67 > *Control-Oriented Models for Real-Time Simulation of Automotive Transmission Systems*
Modélisation orientée-contrôle pour la simulation en temps réel des systèmes de transmission automobile
N. Cavina, E. Corti, F. Marcigliano, D. Olivi and L. Poggio

91 > *Combustion Noise and Pollutants Prediction for Injection Pattern and Exhaust Gas Recirculation Tuning in an Automotive Common-Rail Diesel Engine*
Prédiction du bruit de combustion et des polluants pour le réglage des paramètres d'injection et de l'EGR *(Exhaust Gas Recirculation)* dans un moteur Diesel *Common-Rail* pour l'automobile
I. Arsie, R. Di Leo, C. Pianese and M. De Cesare

111 > *Investigation of Cycle-to-Cycle Variability of NO in Homogeneous Combustion*
Enquête de la variabilité cycle-à-cycle du NO dans la combustion homogène
A. Karvountzis-Kontakiotis and L. Ntziachristos

125 > *Energy Management Strategies for Diesel Hybrid Electric Vehicle*
Lois de gestion de l'énergie pour le véhicule hybride Diesel
O. Grondin, L. Thibault and C. Quérel

143 > *Integrated Energy and Emission Management for Diesel Engines with Waste Heat Recovery Using Dynamic Models*
Une stratégie intégrée de gestion des émissions et de l'énergie pour un moteur Diesel avec un système WHR *(Waste Heat Recovery)*
F. Willems, F. Kupper, G. Rascanu and E. Feru

159 > *Development of Look-Ahead Controller Concepts for a Wheel Loader Application*
Développement de concepts d'une commande prédictive, destinée à une application pour chargeur sur pneus
T. Nilsson, A. Fröberg and J. Åslund

179 > *Design Methodology of Camshaft Driven Charge Valves for Pneumatic Engine Starts*
Méthodologie pour le design des valves de chargement opérées par arbre à cames
M.M. Moser, C. Voser, C.H. Onder and L. Guzzella

195 > *Design and Evaluation of Energy Management using Map-Based ECMS for the PHEV Benchmark*
Conception et évaluation de la gestion de l'énergie en utilisant l'ECMS (stratégie de minimisation de la consommation équivalente) basée sur des cartes, afin de tester les véhicules hybrides électriques rechargeables
M. Sivertsson and L. Eriksson

IFP Energies nouvelles

Oil & Gas Science and Technology – Rev. IFP Energies nouvelles, Vol. 70 (2015), No. 1, pp. 195-211

DOI: 10.2516/ogst/2014018

IFP Energies nouvelles International Conference
Rencontres Scientifiques d'IFP Energies nouvelles

E-COSM'12 - IFAC Workshop on Engine and Powertrain Control, Simulation and Modeling
E-COSM'12 - Séminaire de l'IFAC sur le contrôle, la simulation et la modélisation des moteurs et groupes moto-propulseurs

Design and Evaluation of Energy Management using Map-Based ECMS for the PHEV Benchmark

Martin Sivertsson* and Lars Eriksson

Vehicular Systems, Dept. of Electrical Engineering, Linköping University, 581 83 Linköping - Sweden
e-mail: marsi@isy.liu.se - larer@isy.liu.se

* Corresponding author

Abstract *— Plug-in Hybrid Electric Vehicles (PHEV) provide a promising way of achieving the benefits of the electric vehicle without being limited by the electric range, but they increase the importance of the supervisory control to fully utilize the potential of the powertrain. The winning contribution in the PHEV Benchmark organized by IFP Energies nouvelles is described and evaluated. The control is an adaptive strategy based on a map-based Equivalent Consumption Minimization Strategy (ECMS) approach, developed and implemented in the simulator provided for the PHEV Benchmark. The implemented control strives to be as blended as possible, whilst still ensuring that all electric energy is used in the driving mission. The controller is adaptive to reduce the importance of correct initial values, but since the initial values affect the consumption, a method is developed to estimate the optimal initial value for the controller based on driving cycle information. This works well for most driving cycles with promising consumption results. The controller performs well in the benchmark; however, the driving cycles used show potential for improvement. A robustness built into the controller affects the consumption more than necessary, and in the case of altitude variations the control does not make use of all the energy available. The control is therefore extended to also make use of topography information that could be provided by a GPS which shows a potential further decrease in fuel consumption.*

Résumé — Conception et évaluation de la gestion de l'énergie en utilisant l'ECMS (stratégie de minimisation de la consommation équivalente) basée sur des cartes, afin de tester les véhicules hybrides électriques rechargeables — Les véhicules électriques hybrides rechargeables (PHEV, *Plug-in Hybrid Electric Vehicles*) représentent un moyen prometteur d'obtenir les avantages des véhicules électriques, sans être limités par les problèmes d'autonomie, mais ils augmentent l'importance de la supervision énergétique, afin d'exploiter pleinement le potentiel du groupe motopropulseur. La contribution gagnante au benchmark PHEV, organisé par IFP Energies nouvelles, est décrite et évaluée ici. Le contrôle est réalisé par le biais d'une stratégie adaptative basée sur une approche ECMS (*Equivalent Consumption Minimization Strategy*, stratégie de minimisation de la consommation équivalente) à base de cartographies, développée et mise en application dans le simulateur fourni pour le benchmark PHEV. Le contrôle mis en œuvre s'efforce d'être aussi proche que possible d'une stratégie « *blended* », tout en s'assurant que toute l'énergie électrique est utilisée dans une mission de conduite. Le contrôleur est adaptatif, afin de réduire l'importance de valeurs initiales correctes, mais les valeurs initiales affectant la consommation, une méthode est développée afin d'estimer la valeur initiale optimale pour le contrôleur, sur la base d'informations du cycle de conduite.

Cela fonctionne bien pour la plupart des cycles de conduite et les résultats sont prometteurs en matière de consommation. Le contrôleur fonctionne bien dans le benchmark ; toutefois, les cycles de conduite utilisés montrent qu'un potentiel d'amélioration existe. La robustesse intégrée au contrôleur affecte la consommation plus que nécessaire et en cas de variations d'altitude, le contrôle n'utilise pas toute l'énergie disponible. Le contrôle est donc étendu pour utiliser également les informations topographiques qui pourraient être fournies par un GPS, ce qui conduit à un potentiel de diminution ultérieure de la consommation de carburant.

NOMENCLATURE

r_{wh}	Wheel radius (m)
J_{veh}	Driveline moment of inertia at the wheels (kg m^2)
m_{veh}	Vehicle mass (kg)
g	Gravitational acceleration (m/s^2)
θ	Road slope (rad)
v	Vehicle speed (m/s)
$c_{v,0-2}$	Longitudinal vehicle model parameters (N, Ns/m, Ns^2/M^2)
U_{oc}	Open-circuit voltage (V)
R_c	Internal resistance (Ω)
Q_0	Battery capacity (As)
Q_{tot}	Energy capacity of the battery (J)
SOC	State of Charge (–)
ρ_f	Fuel density (kg/m^3)
q_{LHV}	Lower heating value of the fuel (J/kg)
$\dot{m}_f$	Fuel massflow (kg/s)
m_f	Fuel consumption (L/100 km)
m_{ech}	Fuel equivalent of consumed electricity (L/100 km)
h_{neg}	Height meters downhill in the driving cycle (m)
c_{1-3}	Position of clutch 1-3 (–)
T	Torque (Nm)
ω	Angular velocity (rad/s)
P	Power (W)
η	Efficiency (–)
I	Current (A)
γ	Gear ratio (–)
D_{tot}	Estimated driving cycle distance (km)
D_{real}	Actual distance traveled (km)
n_{on}	Number of engine starts (–)

SUBSCRIPTS

ENG	Engine
GEN	Generator
EM	Electric Motor
GENSET	Engine-generator combination (Mode 3)
rs	Ring-sun
fd	Final drive
wh	Wheel
gb	Planetary gear box
req	Requested
s	Sun wheel of planetary gear box
r	Ring wheel of planetary gear box
c	Carrier wheel of planetary gear box
f	Fuel
b	At the terminal of the battery
ech	Electrochemical, inside the battery
$f \rightarrow ech$	Fuel to electrochemical
avg	Average

CONTROL PARAMETERS

SOC_c	SOC reference
$dSOC$	Allowed deviation from reference
$dSOC_{max/min}$	Maximum and minimum allowed $dSOC$
SOC_f	Final SOC reference
$SOC_{f,0}$	Final SOC reference with adaptive SOC_f
SOC_0	Initial SOC
t_{on}/t_{off}	Thresholds for changing the engine state
λ	Equivalence factor, relating fuel and electricity
λ_c	Center of the λ-control
$\lambda_{c,init}$	Initial λ_c
$\lambda_{c,init,mod}$	Modeled initial λ_c
$l_{l,s}$	Shape parameters of the tan-function
$k_{p,i}$	Gains for the λ_c control
k_{1-5}	Parameters for the $\lambda_{c,init,mod}$ estimation
D_x	Corrected actual distance driven

INTRODUCTION

A Hybrid Electric Vehicle (HEV) utilizes both electric energy and energy from fuel to meet the demands set

by the driver. This may lead to a reduction in the environmental impact and fuel consumption of the vehicle. A Plug-in Hybrid Electric Vehicle (PHEV) is a HEV with the possibility of recharging the battery from the grid. This adds the potential of using the vehicle as an electric vehicle, without the range limitations in a pure electric vehicle. The supervisory control algorithm for these more complex powertrains plays an important role in achieving the full potential of the powertrain. In order to evaluate different strategies, IFP Energies nouvelles (IFPEN) organized a benchmark for the energy management of a PHEV [1, 2] held at the E-COSM'12 - IFAC Workshop on Engine and Powertrain Control, Simulation and Modeling in Rueil-Malmaison near Paris, France.

This paper describes the design, and evaluates the performance of the best-performing controller in the PHEV benchmark problem. As such, the paper describes and also contributes with discussions about several engineering trade-offs that were necessary to make, in order to provide a complete and efficient solution for the benchmark problem. This paper is an extension of [3] where the control strategy was outlined. The control is an extension of the adaptive map-based Equivalent Consumption Minimization Strategy (ECMS) developed in [4] for the PHEV problem and it is implemented for the simulator made available in the PHEV Benchmark.

The PHEV problem poses additional problems compared with HEV control since the control should no longer try to maintain the battery State of Charge (SOC) around a constant reference value. This is since it is desirable to make use of all the stored energy in the battery, the engine should only be started if the driving mission exceeds the electric range of the vehicle. Therefore the control strategy in [4] is extended to also handle a time-varying SOC reference as well as estimation of initial control values from driving cycle data provided in the simulator.

To achieve optimal results using ECMS the optimal value of an equivalence factor needs to be found [5]. However, this optimal value is driving cycle-specific and has to be approximated online. Two promising approaches are found in the literature. Both approaches use a cycle independent-equivalence factor and a correction based on the deviation of SOC from its reference value, denoted SOC error. In [5], the correction is a linear function in SOC error. In [6], the equivalence factor is corrected with a product of two terms, a cubic function of the SOC error and tanh of the low-pass filtered SOC error.

The contribution of the method proposed here is an efficient way of solving and implementing the ECMS control strategy for a PHEV that is also self-contained, using driving distance and average speed to estimate the initial equivalence factor and then adapting it continuously throughout the driving mission to ensure that it is robust to unknown driving missions and that the desired discharge profile is followed.

The main contributions of the paper are the evaluation of the performance in the benchmark, a discussion on the influence of some of the design choices, and finally, the extension of the control to incorporate topology information from GPS to improve the performance in the presence of altitude variations in the driving missions.

1 OUTLINE

In Section 2, the benchmark is presented and the models in the simulator are briefly described. In Section 3, the problem to be solved is formulated and in Section 4, the offline optimization is described. Section 5 describes the architecture of the controller, and the energy management is described in Section 6. Section 7 evaluates the controller's performance in the benchmark and the influence of some of the design choices is discussed in Section 8. Section 9 then suggests some improvements for the controller before the concluding remarks in Section 10.

2 IFPEN PHEV BENCHMARK

In the IFPEN PHEV Benchmark, a simulator is provided for which a supervisory control algorithm is to be designed. This simulator is a quasi-static model of the *Chevrolet* Volt with vehicle and battery dynamics and all energy converters modeled using stationary maps. The architecture of the vehicle and connections between components are shown in Figure 1. The *Chevrolet* Volt has three energy converters, an internal combustion engine (ENG), an Electric Motor (EM) and a generator (GEN), connected through a planetary gear set (GB). Both electric machines can work in both motoring and generating mode. The powertrain also incorporates three clutches that allow the vehicle to be driven in the following four modes:

- Mode 1: one-motor pure electric vehicle. Only the EM is connected to the GB;
- Mode 2: two-motor pure electric vehicle. Both the EM and GEN are connected to the GB;
- Mode 3: series HEV. Only the EM is connected to the GB. The ENG and GEN work as an auxiliary power unit, producing electric power;

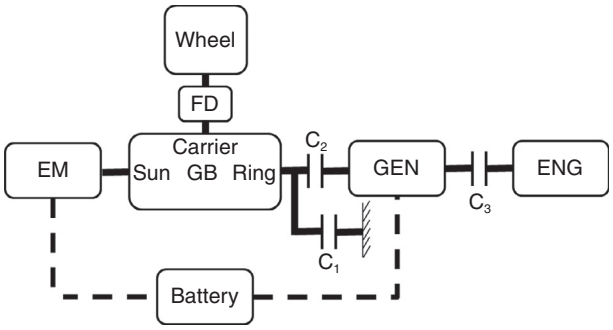

Figure 1

Architecture of the modeled vehicle and the connections between the components.

– Mode 4: power-split HEV. All energy converters are connected to the GB.

In the benchmark, the controller should output desired torque from the ENG, EM and mechanic brakes, the speed of the GEN, the position of the three clutches, and if the engine should be on or off. The inputs to the controller are the requested torque from the driver model, T_{req}, minimum allowed regenerative torque, SOC, vehicle speed, average speed in the driving cycle, v_{avg}, and approximate driving cycle length, D_{tot}. The aim of the control is to minimize the criteria described in Table A1 in Appendix with a battery that is fully charged at the beginning of the driving cycle and may be depleted at the end of the driving cycle. There are also rules on how closely the controller has to follow the desired velocity profile [1].

2.1 Models

The model is provided as a Matlab/Simulink file. The key model equations in the simulator are briefly described below, while the interested reader is referred to [1] for more details.

2.1.1 Vehicle Model

The vehicle motion equation is implemented as (1) where T_{wh} is the torque from the powertrain at the wheels, T_b is the torque applied by the brakes, and v is the vehicle speed:

$$\frac{dv}{dt} = \frac{r_{wh}}{j_{veh}} \times \left(T_{wh} - T_b - r_{wh}\left(m_{veh}\, g \sin\theta + c_{v,0} + c_{v,1} v + c_{v,2} v^2\right)\right) \quad (1)$$

2.1.2 Battery Model

The battery model is of equivalent circuit type with a voltage source and internal resistance and implemented as:

$$I_b = \frac{U_{oc}(SOC)}{2R_c} - \sqrt{\frac{U_{oc}(SOC)^2 - 4R_c P_b}{4R_c^2}} \quad (2)$$

$$P_{ech} = I_b\, U_{oc}(SOC) \quad (3)$$

$$\Delta SOC = -dt \frac{I_b}{Q_0} \quad (4)$$

2.1.3 Transmission

The transmission is a planetary gear set with three clutches, c_1, c_2 and c_3. The kinematic relations between the energy converters and the wheels given by the simulator are:

$$\omega_{ENG} = \omega_{GEN} c_3 \quad (5)$$

$$\omega_{EM} = \omega_{wh}\gamma_{fd}(1+\gamma_{rs}) - \omega_{GEN}\, c_2(1-c_1)\gamma_{rs} \quad (6)$$

$$T_s = T_{EM}\eta_{gb}^{\mathrm{sgn}(T_{EM})} \quad (7)$$

$$T_r = T_s\, \gamma_{rs}\, c_2\, \eta_{gb}^{\mathrm{sgn}(T_s)} \quad (8)$$

$$T_{GEN} = T_r - c_3 T_{ENG} \quad (9)$$

$$T_c = (1+\gamma_{rs})\left((1-c_2)T_s + \frac{c_2}{\gamma_{rs}}(T_{GEN} + c_3 T_{ENG})\right) \quad (10)$$

$$T_{wh} = T_c\, \eta_{gb}^{\mathrm{sgn}(T_c)} \gamma_{fd} \quad (11)$$

2.1.4 Consumption

There are two consumptions provided in the simulator and used in this paper; fuel consumption and a fuel equivalent of the electricity consumption. They are defined as:

$$D_{real} = \int \frac{v}{1000} \quad (12)$$

$$m_f = \frac{\int \dot{m}_f}{\rho_f\, D_{real}} 10^5 \quad (13)$$

$$m_{f,equiv} = \frac{\int P_{ech}}{\eta_{f\to ech}\; q_{LHV}\rho_f D_{real} 10^5} \quad (14)$$

where $\dot{m}_f$ is the fuel flow, ρ_f is the density of the fuel, D_{real} is the distance traveled, P_{ech} is the electrochemical power, $\eta_{f\rightarrow ech}$ is the average efficiency from fuel to electricity and q_{LHV} is the lower heating value of the fuel.

3 PROBLEM FORMULATION

Looking at the scoring metrics and CO_2 data in Tables A1 and A2 the problem can be reformulated as delivering the torque requested by the driver, T_{req}, or as close as possible if the requested torque is infeasible. This should be done in a fuel and computationally efficient way. The performance criteria are actually different measures on torque-tracking ability, therefore they need no further attention than that the controller should follow T_{req} as closely as possible. Even though the specific CO_2 emissions are higher for electricity production, the higher efficiencies of the electric energy converters compared with the efficiency of the combustion engine result in the fact that the minimization of the well-to-wheel CO_2 emissions can be interpreted as fuel consumption minimization. So, the aim is to minimize the energy use, with emphasis on the fuel consumption, while fulfilling the driver's requests. This problem is well accommodated by the ECMS, where the sum of fuel and battery power is minimized. However, battery and fuel power are not directly comparable and therefore an equivalence factor λ relating the two is needed; for more information on ECMS [7-9]. The problem is formulated as:

$$H = P_f + \lambda P_{ech} \tag{15}$$

$$[T_{EM}, T_{ENG}, \omega_{GEN}, Mode] = argmin(H) \tag{16}$$

Subject to:

$$\begin{gathered} T_{wh} = T_{req} \\ T_{i,min}(\omega_i) \leq T_i \leq T_{i,max}(\omega_i) \\ 0 \leq \omega_i \leq \omega_{i,max} \\ i \in [ENG, GEN, EM] \\ P_{b,min}(SOC) \leq P_b \leq P_{b,max}(SOC) \end{gathered} \tag{17}$$

where ω is the rotational speed of the energy converter, and P_b is the power at the terminal of the battery. The torque and speed limits are applied to each individual energy converter.

4 OFFLINE OPTIMIZATION

Since the kinematic relations change with the actuation of the clutches, the optimization problem to be solved differs between the modes. Due to the complex nature of the problem the optimal solution is not calculated online. For a given combination of required torque, wheel speed and equivalence factor (T_{req}, ω_{wh}, and λ), the cost for each mode can be computed. Therefore, in order to find which mode to use when, the minimum cost for each mode is calculated offline, through discretizing the problem and selecting the combination with the lowest cost. The resulting controls are then stored in tables for a given set of (T_{req}, ω_{wh}, and λ). Since the efficiency of the battery does not change much as a function of SOC in the desired operating region of the battery, the SOC is found to only have minor effects on the optimal solution, therefore that effect is ignored.

To ensure that Equation (17) are all fulfilled, or in the case of T_{req} being infeasible, the produced torque is as close to that requested as possible for that mode, the cost function in Equation (15) is augmented so that the closest point, that fulfills all the inequalities is selected.

In order to find which mode is optimal for each combination of T_{req}, ω_{wh} and λ, the optimal torque and speed setpoints also have to be found. However, instead of just storing all the control variables in tables a few insights can be gained from the kinematic relations in Equations (5-11) to reduce the amount of memory used:

- Mode 1: T_{EM} can be calculated from T_{req} in all modes. Therefore, Mode 1 requires no tables;
- Mode 2: only ω_{GEN} has to be stored and since $P_f = 0$ it is independent of λ;
- Mode 3: T_{EM}, ω_{EM}, and therefore P_{EM} are given by T_{req} and ω_{wh}. The optimal output power from the generator should be on the optimal operating line of the engine-generator combination (GENSET). Therefore, only the optimal output power for each P_{EM}, λ combination has to be stored together with the optimal operating line of the GENSET;
- Mode 4: both ω_{GEN} and T_{GEN} or T_{ENG} need to be stored as functions of T_{req}, ω_{wh} and λ.

4.1 Stored Data and Complexity

With the insight from above the following seven tables are stored for the different modes. An example of the resulting tables is also shown in Figure 2. This results in 7 tables to be stored, shown in Figure 2. That is:

- Mode selection (3-D),
- Mode 2: ω_{GEN} (2-D),
- Mode 3: P_{GENSET} (2-D), $\omega_{opt-line}$ (1-D) and $T_{opt-line}$ (1-D),
- Mode 4: ω_{GEN} (3-D) and T_{GEN} (3-D).

The optimization is performed for a dense grid in T_{req}, ω_{wh} and λ. In order to minimize the amount of memory

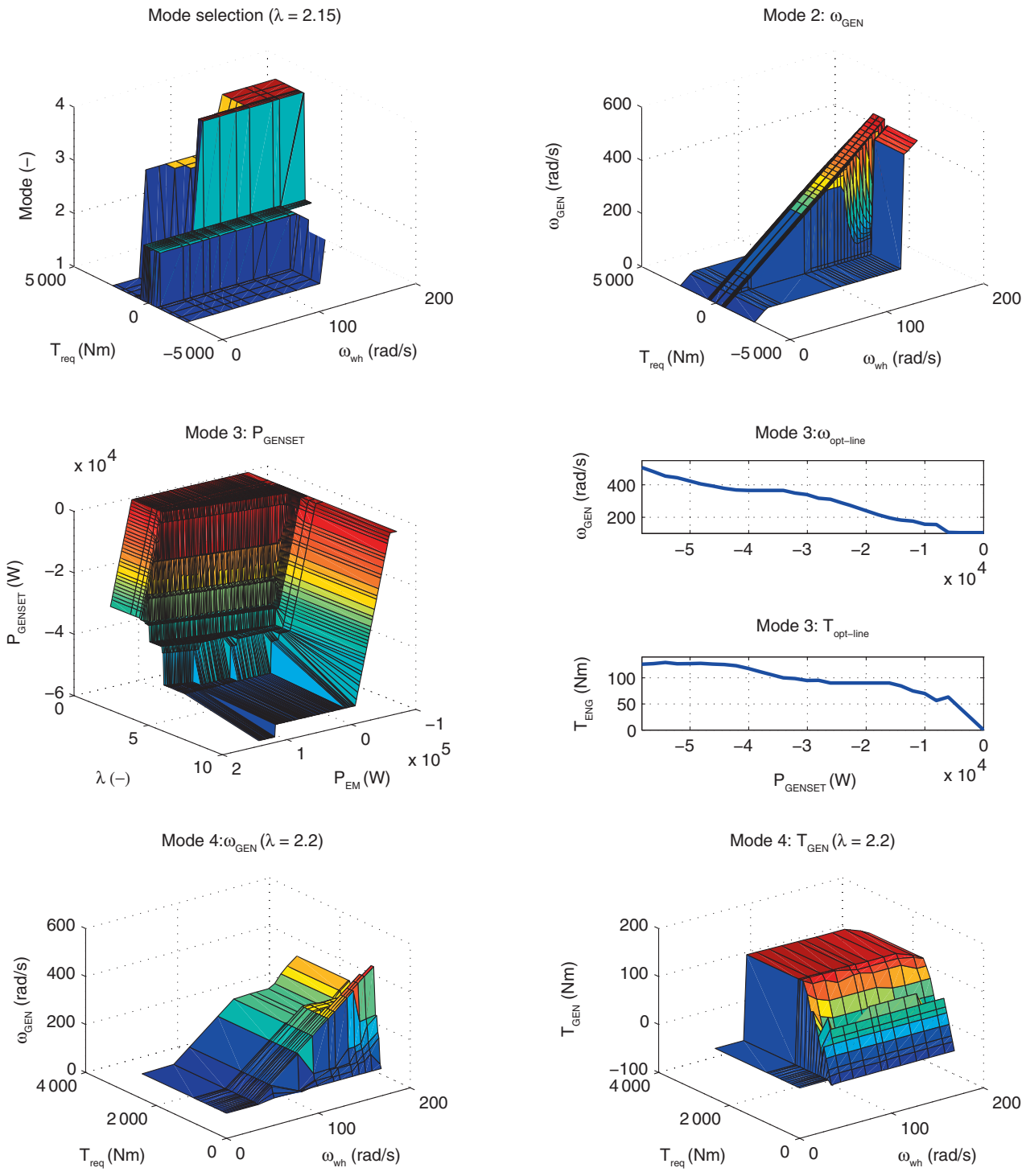

Figure 2

Structure of the stored data, illustrating the complexity of each mode.

used the calculated tables are sparsened in an iterative manner. This means that the T_{req}, ω_{wh} or λ resulting in the smallest error in the interpolation scheme used in the online implementation if removed, is removed in an iterative manner. This is performed for all tables, so each table has its own discretization. To simplify the

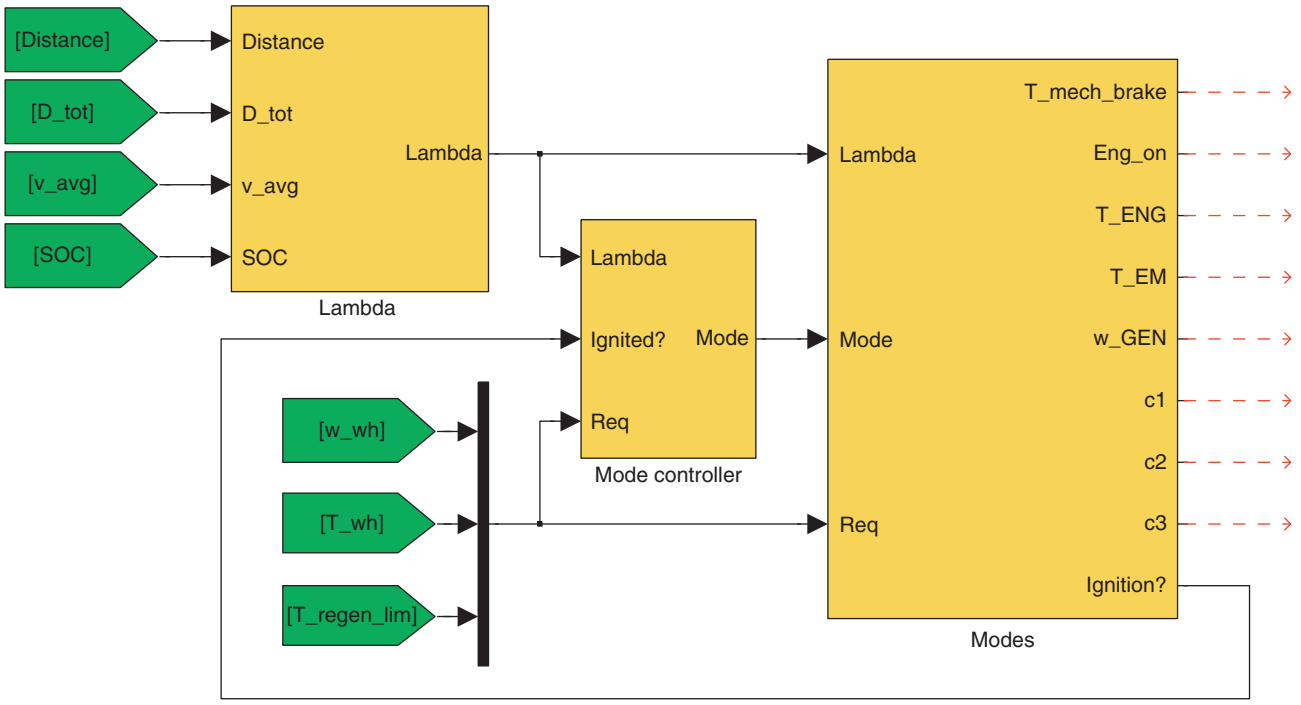

Figure 3

Structure of the controller. The controller consists of three main subsystems, one where the equivalence factor is calculated, one where the mode is selected, and one where the torque and speed setpoints are calculated.

implementation and to reduce the memory consumption Mode 4 is only used when $T_{req} > 0$.

5 CONTROLLER

The basic structure of the controller is shown in a block diagram in Figure 3. The controller consists of three main subsystems. The first subsystem calculates the value of the equivalence factor, λ, using the SOC and driving cycle data, discussed in Section 6.

The second subsystem controls which mode to engage and the third calculates the torque and speed setpoints for the energy converters, both briefly described below.

The mode block consists of five subsystems, one for each mode and one for engine start. The mode controller outputs which mode to activate and if the engine should be started or not. In order to avoid too frequent engine starts/stops, two thresholds are used, t_{on} and t_{off}. The controller has to request engine on/off for a duration longer than $t_{on}/t_{off} = 1/4$ s before it is turned on/off. These values are found heuristically, iterating through several values and driving cycles and selecting the values giving the best performance qualitatively. In the simulator, the transition between modes is instantaneous, except for engine start, which is why no extra penalty or delay on mode switching is implemented. The torques and speed are then calculated using the tables calculated offline and the kinematic relations for that mode defined in Equation (5-11). Care is also taken not to exceed any of the constraints in Equation (17).

6 ENERGY MANAGEMENT

Since the optimal solution is calculated offline and T_{req} and ω_{wh} are outputs from the driver model only λ needs to be decided; λ thus controls the energy management. The energy management of a PHEV is often divided into two categories. The first is to make use of all the stored energy in the battery, that is run as an electric vehicle until the SOC is under a certain limit, and then operates as a hybrid in charge-sustaining mode. This strategy is commonly denoted Charge Deplete-Charge Sustain strategy (CDCS). The main advantage of this strategy is that it is guaranteed to make use of the stored electric energy and does not need information about the future driving mission. The second strategy is to mix usage of

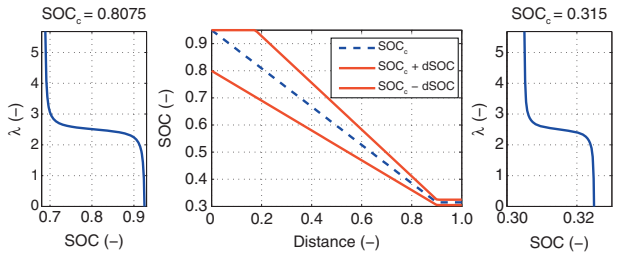

Figure 4

The outline of the basic control shape, λ-function for $D_x \approx 0.2$ (left), SOC_c and $dSOC$ (center) and λ-function for $D_x \geq 0.9$ (right).

fuel and electricity throughout the driving cycle, a strategy known as blended strategy. It is well established in the literature that a blended strategy may result in lower fuel consumption than CDCS [10]. However, in order for a blended strategy to make use of all the energy in the battery the length of the driving cycle has to be known. In the driving cycles provided by the PHEV Benchmark organizers only the approximate distance as well as the mean speed is known. In the provided driving cycles, this approximate distance can deviate from the actual distance of the driving cycle by up to almost 10%.

6.1 Reference SOC

In order to make use of all the stored energy in the battery, a mix between the blended and CDCS strategies is implemented. The strategy is to underestimate the approximate distance by 10%, and use that as a horizon for the blended strategy, then switch to charge-sustaining mode. This is achieved by setting a SOC reference, SOC_c, that is linear in the ratio of traveled distance *versus* expected distance according to Equation (18), a method also used in [6]. The minimum SOC_c, SOC_f, is set to 0.315 in order to ensure that $SOC(end) \geq 0.3$. The shape of SOC_c is shown in Figure 4:

$$\begin{aligned} D_x &= \frac{D_{real}}{0.9D_{tot}} \\ SOC_c &= (SOC_f - SOC_0)D_x + SOC_0 \\ SOC_f &\leq SOC_c \leq SOC_{max} \end{aligned} \tag{18}$$

6.2 Equivalence Factor Adaptation

A common strategy when using ECMS is to adapt the equivalence factor according to an affine function of the SOC error [2, 5]. Here, for robustness reasons, another approach is used. The strategy used in [4] is extended to fit the PHEV problem. The strategy is to adapt the equivalence factor according to a tangent function in SOC. The idea is that as long as the SOC is near the desired SOC the control should remain rather constant; but when the SOC approaches the limits the control needs to adapt. In [4], this is used in a HEV where the aim is to maintain the SOC around a constant level. Here, since it is a PHEV, it is desirable to use the energy stored in the battery, therefore the center of the tan-function is SOC_c. The SOC window used is also decreased linearly with distance traveled. This is to allow larger deviations early in the driving mission, and then make the control follow the SOC_c on a narrower band towards the end of the driving cycle. The λ-adaptation is given by Equation (19), where l_1 and l_s are constants that control the slope and range of the tangent function, and $dSOC$ is the allowed deviation from SOC_c:

$$\begin{aligned} dSOC &= (dSOC_{max} - dSOC_{min})D_x + dSOC_{max} \\ dSOC &\geq dSOC_{min} \\ \lambda &= \lambda_c - l_1 \tan\left(\frac{l_s \pi}{2dSOC}(SOC - SOC_c)\right) \end{aligned} \tag{19}$$

A benefit with this formulation is that the smaller the $dSOC$, the steeper the slope around SOC_c becomes and the faster the control reacts to deviations. In Figure 4, the shape of the control is shown for the case when the approximate distance is correct. That is, the SOC_c undershoots the distance traveled, and thus results in the control going over to charge-sustaining mode. Also shown is that the allowed SOC deviation gets smaller with distance.

The variable λ_c still has to be decided. In Table 1, the change in consumptions compared with the consumptions with optimal λ_c and end SOC are shown for different values of λ_c and different driving cycles. A λ_c is considered optimal if the λ trajectory follows the desired discharge profile, SOC_c. However, since SOC_c is based on undershooting the approximate driving cycle length, there are λ_c values that result in lower consumptions; this is, however, hard to predict. Instead, the optimality of λ_c is qualitatively assessed and the parameter is found in an iterative manner. It is seen that the optimal value changes with the driving cycle. The control ensures $SOC(end) \geq 0.3$ for all λ_c but it might come with a substantial increase in consumption if the λ_c value is wrong.

In Figure 5, the λ and SOC trajectories for the different values of λ_c on 10×US06 driving cycle are shown, as well as the mode selection for the final repetition of the cycle. Due to the driving mission length provided only being approximate, the control undershoots the length in order to make sure all electric energy is used.

TABLE 1
The change in consumptions compared with $\lambda_{c,opt}$ for different values of λ_c. All controls ensure $SOC(end) \geq 0.3$. n_{on} is the number of engine starts

Cycle-info	λ_c	Δm_f (%)	$\Delta m_{f,equiv}$ (%)	SOC(end)	n_{on}
10×FUDS	3	–0.65	–0.19	0.3099	66
D_{tot} = 119.9 km	$\lambda_{c,opt}$ = 2.65	-	-	0.3076	62
D_{real} = 119.9 km	2	10.35	2.32	0.3066	73
10×NEDC	3	27.02	15.87	0.3420	25
D_{tot} = 119.9 km	$\lambda_{c,opt}$ = 2.63	-	-	0.3197	10
D_{real} = 110.1 km	2	0.80	0.56	0.3162	15
10×US06	3	–0.03	–0.71	0.3147	110
D_{tot} = 119.9 km	$\lambda_{c,opt}$ = 2.85	-	-	0.3103	125
D_{real} = 128.9 km	2	5.30	2.20	0.3078	130

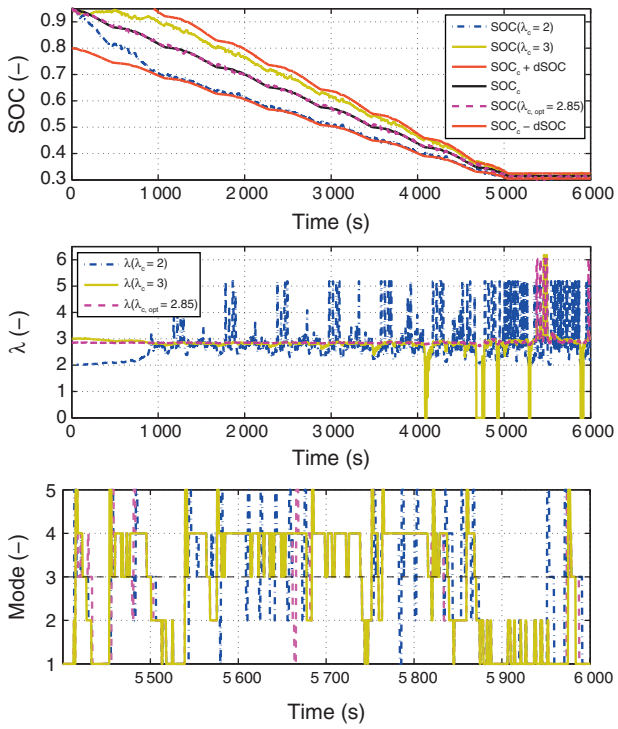

Figure 5

The SOC and λ-trajectories for different λ_c values on 10×US06 driving cycle as well as the modes used for the last repetition of US06. Mode = 5 represents engine start. A poor λ_c may lead to a switching characteristic of the control, which is also visible in the number of engine starts.

The US06 cycle is, however, 7% longer than the length provided, resulting in an undershoot of roughly 16% for the controller. It is seen that the control for $\lambda_c \neq \lambda_{c,opt}$ does not follow the SOC_c; instead it follows $SOC_c \pm dSOC$. For $\lambda_c = 2$ this results in a control that switches rapidly between $\lambda \approx 2.5$ and $\lambda \approx 5$, something that comes with a large consumption penalty. It also affects the number of engine starts, seen in Table 1.

6.3 Adaptive Control of λ_c

In order to avoid the switching nature of the λ-control seen in Figure 5 the idea is to adapt λ_c if the SOC deviates too much from SOC_c. This is done with a PI controller according to:

$$\lambda_c = \lambda_{c,init} + K_p(SOC_c - SOC) + K_i \int (SOC_c - SOC)dt \tag{20}$$

where K_p and K_i control how fast the controller adapts, but a faster controller comes with a slight consumption penalty. In Table 2, the consumption change compared with $\lambda_{c,opt}$ for adaptive λ_c is shown for different driving cycles and $\lambda_{c,int}$. The number of engine starts is also shown. A $\lambda_{c,init}$ is considered optimal if it roughly produces a SOC trajectory that follows the desired trajectory without λ_c deviating too far from $\lambda_{c,init}$, *i.e.* producing a roughly constant λ trajectory. This value is, as with $\lambda_{c,opt}$, qualitatively assessed and found in an iterative manner. It is seen that the adaptive λ_c performs as well as $\lambda_{c,opt}$, better in some cases, worse in some cases, but most of all it reduces the effect of poor initial values. This is also confirmed in Figure 6, where the SOC and λ trajectories are shown for 10×US06 driving cycle, as well as the mode selection for the final repetition of the cycle.

TABLE 2

The change in consumption with adaptive λ_c for different $\lambda_{c,init}$, compared with $\lambda_{c,opt}$. n_{on} is the number of engine starts

Cycle-info	$\lambda_{c,init}$	Δm_f (%)	$\Delta m_{f,equiv}$ (%)	SOC(end)	n_{on}
10×FUDS	3	0.10	–0.29	0.3110	68
D_{tot} = 119.9 km	$\lambda_{c,init,opt}$ = 2.65	–0.57	–0.05	0.3075	61
D_{real} = 119.9 km	2	–0.87	–0.16	0.3081	57
10×NEDC	3	15.61	0.45	0.3306	22
D_{tot} = 119.9 km	$\lambda_{c,init,opt}$ = 2.55	–0.16	0.08	0.3188	10
D_{real} = 110.1 km	2	1.69	0.45	0.3184	16
10×US06	3	0.07	–0.41	0.3143	125
D_{tot} = 119.9 km	$\lambda_{c,init,opt}$ = 2.85	0.03	–0.18	0.3109	125
D_{real} = 128.9 km	2	0.39	–0.05	0.3101	119

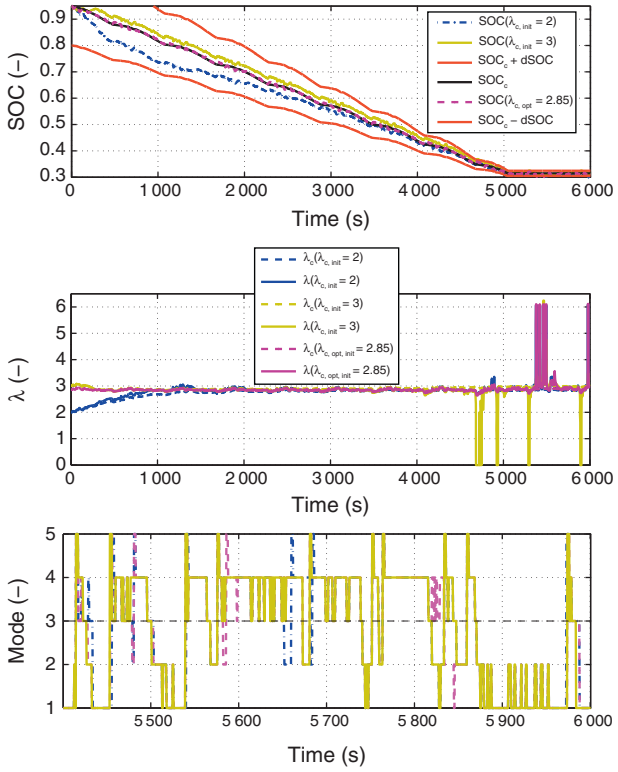

Figure 6

The SOC and λ trajectories with adaptive λ_c for different values on $\lambda_{c,init}$ on 10×US06 driving cycle as well as the modes used for the last repetition of US06. Mode = 5 represents engine start. The adaptive λ_c reduces the effect of poor initial values.

The switching nature is almost completely removed, resulting in a nearly constant λ value during the entire blended phase.

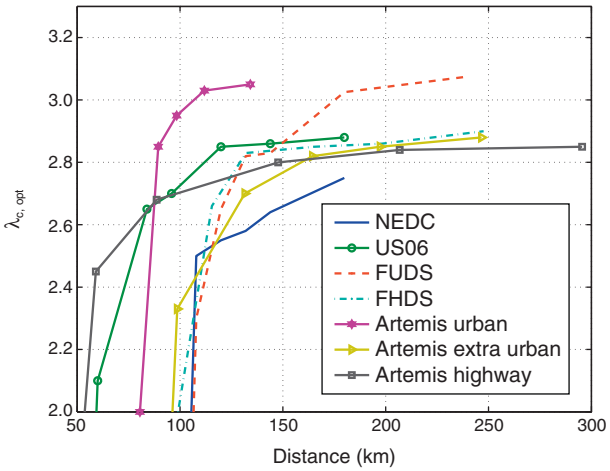

Figure 7

The optimal $\lambda_{c,init}$ as a function of approximate distance for different driving cycles. The general shape of the curves are similar; however, the all-electric range differs among the cycles.

6.4 Estimating $\lambda_{c,init}$

Although the developed control has been seen to perform well for all reasonable initial λ_c, the consumption is still affected by it. Therefore, it is desirable to achieve an estimate as close as possible to the optimal λ_c. In Figure 7, the optimal $\lambda_{c,init}$ is plotted against approximate distance for the driving cycles used. It is seen that the shape of the profiles is similar for all driving cycles. The all-electric range, seen in Figure 7 as $\lambda_{c,init} \geq 2$, differs up to almost 100% for the different driving cycles.

In Figure 8, the approximate distance required to exceed the all-electric range is plotted against mean speed. Even if the mean speed is not enough to describe the driving cycle, since neither the slope nor how transient it is are captured by the mean speed, the all-electric range is approximated by a linear function, shown in Figure 8. Artemis Urban is plotted in magenta to mark that it is considered an outlier and is not included when the line is fitted. Since the losses in the vehicle motion Equation (1) are quadratic in speed, a straightforward assumption would be that the all-electric range decreases with mean speed, an assumption that is also used here. The approximate distance is then corrected with the proposed linear correction, in order to compensate for the different all-electric ranges. The result is shown in Figure 9. It is seen that the correction shifts the points to the same region, a trend that is well captured by an exponential function. The final scheme to estimate $\lambda_{c,init}$ is of the form:

$$D_{corr} = D_{tot} - \left(k_1 v_{avg} + k_2\right) \tag{21}$$

$$\lambda_{c,init,mod} = k_3(1 - \exp(-k_4 D_{corr} + k_5)) \tag{22}$$

In Table 3, the results for the full controller with $\lambda_{c,init,mod}$ are compared with the results for $\lambda_{c,init,opt}$. Even if the estimated $\lambda_{c,init}$ is not too far from the optimal, the consumption can differ substantially. Interesting to note is that the driving cycle with the largest $\lambda_{c,init}$ error shows the best result. Looking at Figure 10, this appears to be due to the $\lambda_{c,init,mod}$-control that has a higher λ value when entering charge-sustaining mode which results in less switching behavior and lower consumption.

Another important property of the $\lambda_{c,init}$ estimation is that it should be such that it avoids unnecessary engine starts if the driving mission is within the all-electric range. This is achieved for all tested driving cycles except FHDS (1 unnecessary start) and Artemis Extra-Urban (2 unnecessary starts), which is deemed acceptable.

7 BENCHMARK EVALUATION

In the PHEV Benchmark, the controller is tested on two unknown driving cycles, hence not used in the design of

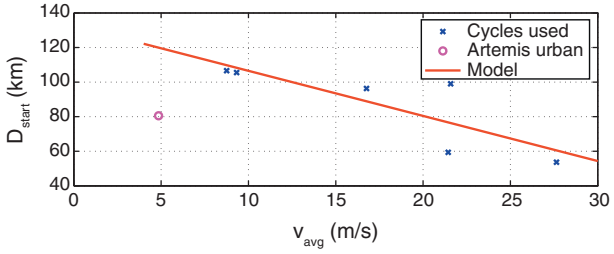

Figure 8

The approximate distance required to exceed the all-electric range for different driving cycles and a linear model to capture the behavior. Artemis urban is considered an outlier and is not included when the line is fitted.

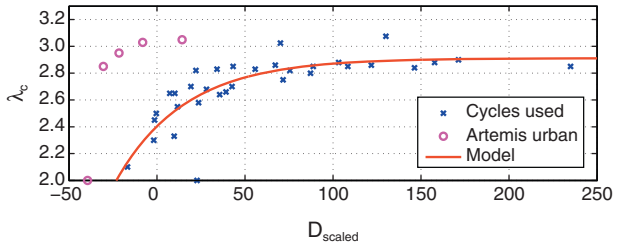

Figure 9

$\lambda_{c,init,opt}$ *versus* corrected approximate distance and how it is modeled. Artemis urban is considered an outlier and is not included when the curve is fitted.

TABLE 3

The change in consumption with $\lambda_{c,init,mod}$, compared with $\lambda_{c,init,opt}$. n_{on} is the number of engine starts

Cycle-info	$\lambda_{c,init,mod}$	Δm_f (%)	$\Delta m_{f,equiv}$ (%)	$SOC(end)$	n_{on}
10×FUDS ($\lambda_{c,init,opt}$ = 2.65)	2.518	13.62	2.32	0.3066	65
10×NEDC ($\lambda_{c,init,opt}$ = 2.55)	2.533	0.80	0.56	0.3162	12
10×US06 ($\lambda_{c,init,opt}$ = 2.85)	2.741	5.30	2.20	0.3078	124
20×Artemis urban ($\lambda_{c,init,opt}$ = 2.84)	2	–6.69	–1.41	0.3104	105

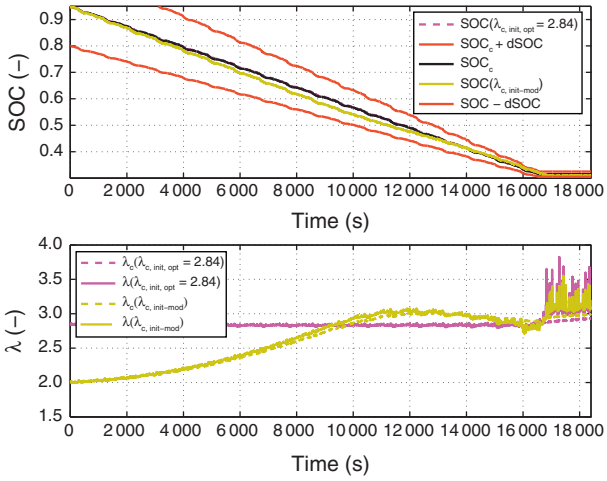

Figure 10

SOC and λ trajectories for the full controller, with $\lambda_{c,init,mod}$, compared with $\lambda_{c,init,opt}$. The modeled $\lambda_{c,init}$ is quite far from the optimal but still $SOC(end) \geq 0.3$.

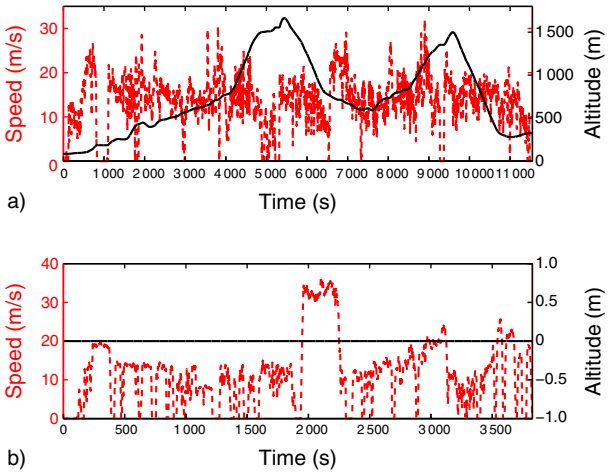

Figure 11

The two driving cycles used in the benchmark. a) Arco-Merano, b) Aachen.

TABLE 4

Benchmark results for the developed controller

Metric	Arco-Merano	Aachen
Total energy use (fuel + electricity) (MJ/km)	1.0809	0.8664
Fuel consumption (MJ/km)	0.9259	0.5913
Well-to-wheel CO_2 emissions (kg/km)	0.0942	0.0768
Processor use (s)	2.9874	2.9631
Memory use (MB)	0.1535	
Acceleration 70-120 km/h (s)	9.1	
Acceleration 0-100 km/h (s)	7.3	
Acceleration 0-1 000 m on 4% slope (s)	32.6	
Braking distance from 100 km/h (m)	37.7614	

the controller (*Fig. 11*). Both cycles are rather transient and the first cycle, Arco-Merano, has substantial altitude variations, whereas the second, Aachen, is on flat road. The results for the benchmark tests are shown in Table 4. For both tested cycles the controller performs relatively well and is close to the solution predicted by HOT, described in [5]. The results are within 3.6% in fuel consumption. This is despite the fact that the controller is implemented without knowledge of the future driving profile and road slope and with a memory usage of just 154 kB. For a closer comparison between the resulting controls and the solution predicted by HOT see [2].

The resulting SOC and λ trajectories for the tested cycles are shown in Figure 12. For both cycles D_{tot} is accurate and therefore the SOC_c reference has both a blended and a charge sustaining phase. For Aachen, it is seen that the controller performs well, the $\lambda_{c,init}$ is fairly close to the desired λ-region and the control manages to maintain SOC near SOC_c during the entire blended phase without large variations in λ. During the charge-sustaining phase the control becomes a bit switching to maintain SOC within the desired window.

For Arco-Merano, it is apparent that a linear discharge profile is not optimal. This is since the altitude

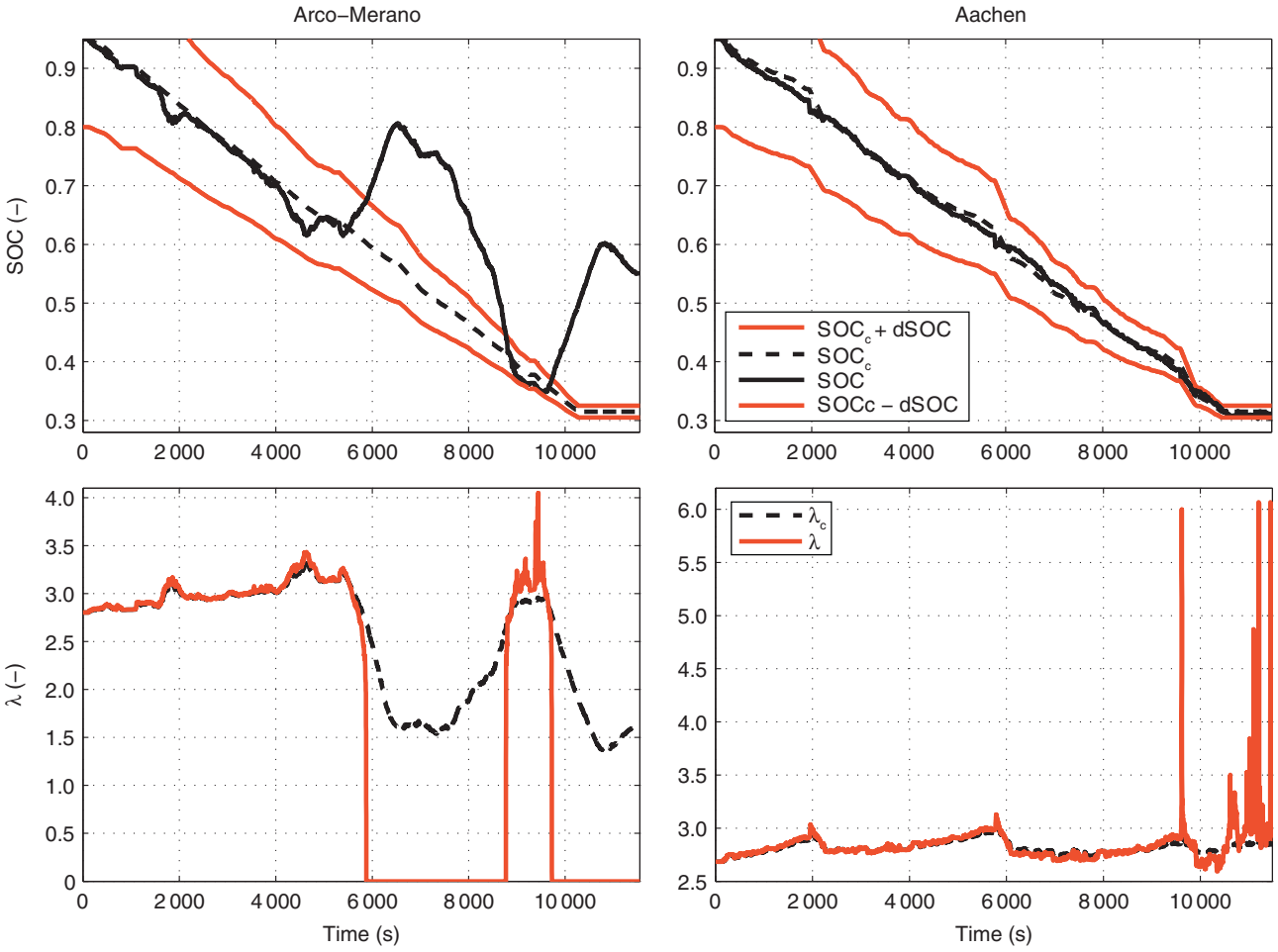

Figure 12

The SOC and λ trajectories for the two cycles used in the benchmark.

variations, or more accurately the road slope, acts as a disturbance and is unknown to the controller. During the first uphill the control works as expected, maintaining the SOC near SOC_c, but during the subsequent downhill phase the recuperation moves SOC outside the desired SOC window. In the second uphill phase the control then brings the SOC back into the SOC window, but the final downhill yet again brings the SOC outside of the SOC window.

8 DISCUSSION

The main objective of the controller is to minimize fuel, and one of the basic ideas to accomplish this is to make sure that all the energy in the battery is used. However, since one of the requirements is that $SOC(end) \geq 0.3$ for the entry not to be disqualified, this needs to be taken into account. This is accomplished by underestimating the total distance, setting a SOC target higher than SOC_{min}, and decreasing the allowed deviation from the desired SOC the closer to the end of the cycle the vehicle gets. Using a tan-function can also be considered a safety measure since it is seen in Figure 5 that the tan-function does not make the control follow the desired discharge profile; instead it makes sure that the control stays within the desired SOC window. All these safety measures affect the consumption, but how much and in what way depends on the driving cycle.

For instance, for Arco-Merano, setting $\lambda = \lambda_c$, that is, removing the tan part, improves the fuel economy by 2.9%, but instead for Aachen $SOC(end) < 0.3$. In a real vehicle the lower SOC limit would be more of a soft constraint and this might not be critical. Without perfect

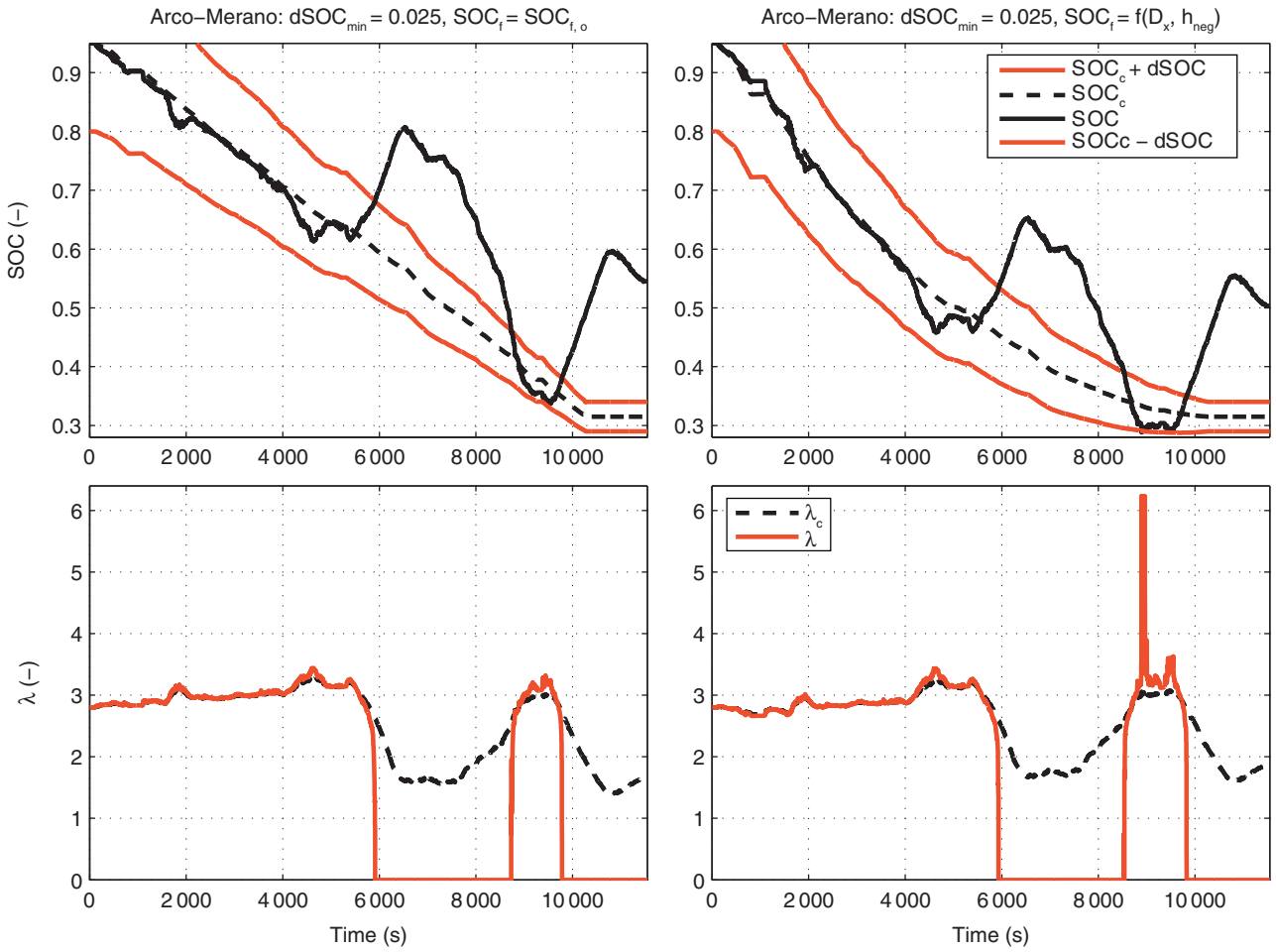

Figure 13

The SOC and λ trajectories for the case with increased $dSOC_{min}$ (left) and with topology taken into account (right), Arco-Merano.

look-ahead the control will potentially end up in charge-sustaining operation and this is something that needs to be handled. One way could be with gain scheduling of the gains in Equation (20), or as here with a tan-function. This is also true for SOC_f. For some cycles, especially with downhill phases, it would be beneficial to set $SOC_f < 0.3$, forcing the controller to follow a steeper discharge profile but then for other cycles $SOC(end) < 0.3$.

Removing the underestimation of driving cycle length is not as trivial since the design of $\lambda_{c,init,mod}$ depends on it. However, since the aim is to minimize fuel consumption, a reasonable assumption is that the fuel penalty of ending with energy left in the battery is larger than the fuel penalty of the strategy not being completely blended, which supports the under-estimation as long as the driving cycle length is not exactly known.

9 CONTROLLER EXTENSIONS

Up until now the focus has been on the controller implementation and design trade-offs that were made for the benchmark. This section describes some extensions that were implemented after the benchmark was completed. Both cycles used in the benchmark evaluation highlight different aspects of potential improvement for the controller. Two suggested improvements for the controller are increasing the allowed SOC window and incorporating topology information, both described in the following subsections.

9.1 Increasing the Allowed SOC Window

For Aachen the control during the charge-sustaining phase switches between $\lambda \approx 3$ and $\lambda \approx 6$, something that

is also visible to a lesser extent in Arco-Merano around 9 000 s, which increases the consumption. This is almost completely removed if $dSOC_{min}$ is increased from 1% to 2.5%, with a corresponding fuel consumption decrease of 2.7% (Aachen) and 0.9% (Arco-Merano). Even with this larger SOC window $SOC(end) > 0.3$ for both cycles, something that also holds for all other tested cycles except 10×FUDS, where $SOC(end) = 0.298$, but in a real application such small deviations might be acceptable.

9.2 Including Topography Information

In Arco-Merano during the downhill segments braking is needed and energy can be recuperated, energy that could be used in the uphill phases. However, to be able to make use of this potential energy some look-ahead is necessary. If the topography is known beforehand and provided to the controller from map and GPS data this could be used in the controller. Vehicle potential energy recuperated in the downhill phases is not taken into account when setting the SOC reference; if estimates of this can be used this could offer potential for improvement. A suggested extension to the control strategy, given that this information is available, is to relate the potential energy to SOC and decrease the target SOC, SOC_f, with the amount of energy that can be expected to be recuperated. The requirement is still that $SOC(end) \geq 0.3$ and therefore SOC_f is increased as a function of the traveled distance. The new SOC_f strategy used together with equation (18) thus becomes:

$$SOC_f = SOC_{f,o} - (1 - D_x)\frac{h_{neg} m_{veh} \eta_{avg} g}{Q_{tot}} \qquad SOC_f \leq SOC_{f,o} \tag{23}$$

In Equation (23), $SOC_{f,o} = 0.315$, h_{reg} is the sum of altitude difference in the downhill phases in the driving cycle, η_{avg} is an estimate of the average efficiency from the wheels to the battery, set to 0.8, and Q_{tot} is the energy capacity of the battery. In the presence of altitude variations this evaluates to a quadratic expression in distance traveled, but on flat road it is equivalent to Equation (18). The results for Arco-Merano with this strategy, as well as the results when just increasing $dSOC_{min}$, are shown in Figure 13.

The resulting trajectories are similar, but as expected the control with varying SOC_f increases the battery usage during the first uphill and therefore ends at a lower SOC, $SOC(end) = 0.5036$ *versus* $SOC(end) = 0.5454$. When $dSOC_{min}$ is increased the switching nature of λ disappears but with the addition of varying SOC_f the switching returns. This is, however, deemed acceptable since the controller still needs to be robust to the other driving cycles. The extra depletion of the battery results in an additional fuel consumption reduction of 4.9%, results that also hold for the other driving cycle with altitude variations provided by the organizers (VAIL2N-REL, 12.4% decrease).

CONCLUSIONS

The design and development of the winning control strategy in the IFPEN PHEV Benchmark is described. The strategy is an adaptive map-based implementation of ECMS striving to be as blended as possible, but still ensuring that all electric energy is used. The controller tries to follow a SOC reference that is linear in traveled distance, but to ensure that all electric energy is used this distance is underestimated. The equivalence factor is adapted according to a function in SOC, a function whose center adapts according to how well the SOC reference is followed. Finally, a method for estimating the initial value for the controller from driving cycle data is developed.

In the benchmark, the controller is seen to perform well, close to the results predicted by HOT. This is despite being implemented just using the approximate driving distance and average velocity. In the case of altitude variations the assumed linear discharge profile is not followed, due to the fact that the slope of the road is unknown to the controller. Also, the allowed SOC window, kept narrow to ensure complete use of the battery energy whilst still ensuring that the final SOC is within the limits prescribed in the benchmark, affects the consumption more than necessary.

The controller is therefore extended, first to be allowed to make use of more of the battery, and finally to incorporate topology if available, a strategy that is seen to perform well with promising consumption results.

REFERENCES

1 PHEV Benchmark Rules (2012) web site: http://www.ecosm12.org/sites/ecosm12.org/files/PHEVbenchmarkrules.pdf. Downloaded 2012-07-18.

2 Sciarretta A., Serrao L., Dewangan P.C., Tona P., Bergshoeff E.N.D., Bordons C., Charmpa L., Elbert Ph., Eriksson L., Hofman T., Hubacher M., Isenegger P., Lacandia F., Laveau A., Li H., Marcos D., Nüesch T., Onori S., Pisu P., Rios J., Silvas E., Sivertsson M., Tribioli L., van der Hoeven A.-J., Wu M. (2013) A controller benchmark on the supervisory control of a plug-in hybrid electric vehicle. Accepted for *Publication in Control Engineering Practice*.

3 Sivertsson M. (2012) Adaptive control using map-based ecms for a phev, *E-COSM'12 – IFAC Workshop on Engine and Powertrain Control, Simulation and Modeling*, Rueil-Malmaison, France, 23-25 Oct.

4 Sivertsson M., Sundström C., Eriksson L. (2011) Adaptive control of a hybrid powertrain with map-based ECMS, In *IFAC World Congress*, Milano, Italy.

5 Chasse A., Hafidi Gh., Pognant-Gros Ph., Sciarretta A. (2009) Supervisory control of hybrid powertrains: an experimental benchmark of offline optimization and online energy management, *E-COSM'09 – IFAC Workshop on Engine and Powertrain Control, Simulation and Modeling*, Rueil-Malmaison, France, 30 Nov.-2 Dec., pp. 109-117.

6 Tulpule P., Marano V., Rizzoni G. (2009) Effects of different PHEV control strategies on vehicle performance, *American Control Conference*, St. Louis, USA.

7 Musardo C., Rizzoni G. (2005) A-ECMS: An adaptive algorithm for hybrid electric vehicle energy management, *IEEE Conference on Decision and Control and the European Control Conference* **44**, 1816-1823.

8 Paganelli G., Delprat S., Guerra T.M., Rimaux J., Santin J. J. (2002) Equivalent consumption minimization strategy for parallel hybrid powertrains, *IEEE Conference on Vehicular Technology* **55**, 2076-2081.

9 Sciarretta A., Back M., Guzzella L. (2004) Optimal control of parallel hybrid electric vehicles, *IEEE Transactions on Control Systems Technology* **12**, 3, 352-363.

10 Larsson V., Johannesson L., Egardt B. (2010) Impact of trip length uncertainty on optimal discharging strategies for phevs, *AAC'10 – IFAC Symposium on Advances in Automotive Control*, Munich, Germany, 12-14 July.

Manuscript accepted in March 2014
Published online in June 2014

Cite this article as: M. Sivertsson and L. Eriksson (2015). Design and Evaluation of Energy Management using Map-Based ECMS for the PHEV Benchmark, *Oil Gas Sci. Technol* **70**, 1, 195-211.

APPENDIX: Benchmark Data

TABLE A1
The scoring metrics used in the benchmark

	Metric	Weight (%)
Performance (30%)	Acceleration 0-100 km/h (s)	7.5
	Acceleration 70-120 km/h (s)	7.5
	Acceleration 0-1000 m on 4% slope (s)	7.5
	Braking distance from 100 km/h (m)	7.5
Energy and economy (50%)	Total energy use (fuel + electricity) (MJ/km)	15
	Fuel consumption (MJ/km)	20
	Well-to-wheel CO_2 emissions (kg/km)	15
Computational performance (20%)	Processor use (simulation time)	10
	Memory use (MB)	10

TABLE A2
Data for CO_2 emissions

Gasoline well-to-tank emissions	12.5 g CO_2/MJ of fuel
Gasoline combustion	73.4 g CO_2/MJ of fuel
Electricity production (Europe average)	94.7 g CO_2/MJ of electric energy